ELSEVIER

Marine Micropaleontology 42 (2001) 189–210

MARINE MICROPALEONTOLOGY

www.elsevier.nl/locate/marmicro

Isotopic composition and morphology of living *Globorotalia scitula*: a new proxy of sub-intermediate ocean carbonate chemistry?

Masashi Itou[a,*], Tsuneo Ono[b], Tadamichi Oba[a], Shinichiro Noriki[a]

[a]*Graduate School of Environmental Earth Science, Hokkaido University, Kita 10 Nishi 5, Sapporo 060-0810, Japan*
[b]*National Research Institute of Fisheries Sciences, Yokohama 236-8648, Japan*

Received 23 March 2000; revised 26 January 2001; accepted 10 February 2001

Abstract

Abundance, isotopic composition and morphological imprints of the planktonic foraminifera *Globorotalia scitula* (Brady) were closely examined for possible use as a novel reconstruction tool of chemical environments in sub-intermediate depth seawater in the past. Based on the MOCNES plankton tow observation of dwelling depths of *G. scitula* and the isotopic compositions together with hydrochemistry data, the empirical relations between isotopic disequilibria in carbon ($\Delta\delta^{13}C = \delta^{13}C_{G.\ scitula} - \delta^{13}C_{DIC}$) and oxygen ($\Delta\delta^{18}O = \delta^{18}O_{G.\ scitula} - \delta^{18}O_w$) isotopes in the carbonate tests and the seawater $\delta^{18}O$ and $\delta^{13}C$ of dissolved inorganic carbon (DIC), respectively, are introduced. The morphological information such as pore density and porosity is also examined for significant relations to carbonate chemistry. Shell porosity is strongly correlated saturation state of calcite. The dissolution of living *G. scitula* tests may promote the observed isotopic differences as well as the increases in porosity. $\Delta\delta^{18}O$ of *G. scitula* is found effectively to be linear function of both water temperature and calcite saturation state (Ω), and thereby temperature equation for *G. scitula* is provided, while $\Delta\delta^{13}C$ of *G. scitula* is a linear function of only calcite saturation state.

The equation was validated by using *Globorotalia scitula* collected by a sediment trap in intermediate water depths. Satisfactory agreements were found between observed and calculated $\Delta\delta^{18}O$ from the empirical equations based on temperature and hydrochemistry data at sediment trap deployment site, indicating that the equation may be useful in paleo-environmental reconstruction of sub-intermediate water. The sediment trap observation further suggests that the abundance of *G. scitula* does not necessarily correspond to surface water productivity and to POC flux, but instead, it correlates well with the supply of fine organic matter, which appears to be a result of water convection. Thus, *G. scitula* may be an unambiguous and excellent paleo-environmental recorder for carbonate chemistry and for fine organic matter transport to the depths, if isotopic and morphological observations are combined.

Keywords: foraminifera; *Globorotalia scitula*; morphology; isotopes; carbonate chemistry

1. Introduction

Numerous studies have shown the existence of well-ventilated intermediate water in the glacial ocean (Lynch-Stieglitz and Fairbanks, 1994; Lynch-Stieglitz et al., 1996; Marchitto et al., 1998). Today's North Pacific Intermediate Water (NPIW) is distributed around $\sigma_\theta = 26.8 - 27.2$ (Reid, 1965; Yasuda, 1997), and this water mass is distinguished as a

* Corresponding author. Fax: +81-11-706-2247.
E-mail address: f073406@ees.hokudai.ac.jp (M. Itou).

0377-8398/01/$ - see front matter
PII: S0377-8398(01)00015-9

salinity minimum. The NPIW seems to originate in the Sea of Okhotsk, where sea ice formation leads to the creation of dense shelf waters (Sverdrup et al., 1942; Tally, 1991; Yasuda et al., 1996). Changes in sea ice formation during the glacial period might have no small effect on the behavior of sub-surface and intermediate water circulation in the past North Pacific (Shiga and Koizumi, 2000). Although much progress in paleoceanographic studies has been made on the continental margin sediments in the Pacific (Keigwin, 1998; Kwiek and Ravelo, 1999), we still have only a few proxies (Lohmann and Schweitzer, 1990) for reconstructing the past sub-intermediate depth (ca. $<$1000 m) environment, especially in the open ocean.

Ice core records indicate that atmospheric CO_2 concentration was lower in the glacial period than the present (e.g. Petit et al., 1999). Several hypotheses have been proposed to explain this evidence (e.g. Martin, 1990). Recently, the high pH and high carbonate ion concentration in the glacial ocean has been proposed as a cause of this low atmospheric CO_2 (Archer and Maier-Reimer, 1994; Sanyal et al., 1995). However, these studies are focused on the surface and bottom water, and little attention has been paid to the sub-surface and intermediate water. Considerable dissolution of carbonate particles takes place in the upper 500–1000 m of the ocean (Milliman et al., 1999), well above the chemical lysocline. Oba and Pedersen (1999) suggested that during glacial periods, dissolution of fine eolian carbonates in sub-surface waters should have enhanced atmospheric CO_2 absorption by increasing alkalinity. Accordingly, reconstruction of the carbonate chemistry in the sub-intermediate depths would be useful to understand the past carbon cycle. So far, no way has been proposed to reveal the past sub-intermediate water conditions in the open ocean. For these reasons, our understanding of carbonate chemistry in the sub-intermediate water should be increased to reveal how atmospheric CO_2 concentration was controlled in the past.

Globorotalia scitula (Brady) is classified as a polar–sub-polar species (Thunell, 1978; Bé and Tolderlund, 1971). However, its wide geographical distribution has been confirmed in the North Atlantic, the Mediterranean Sea, the Panama Basin, the Indian Ocean, the central equatorial Pacific Ocean, the Sea of Okhotsk, and the Eastern Pacific Ocean (Baumfalk et al., 1987; Hutson, 1977; Belyaeva and Burmistrova, 1998; Hendy and Kennett, 2000; Marchant et al., 1998; Schiebel et al., 1995; Thunell and Reynolds, 1984; Watkins et al., 1996). Therefore, *G. scitula* cannot be considered as an exclusively polar and sub-polar species. The habitat depth of *G. scitula* which ranges between the surface and 1000 m (Bé, 1977; Schiebel et al., 1995; Ortiz et al., 1996) indicates this species may record sub-intermediate environmental conditions. In general, *Globorotalia* is a solution-resistant genus (Parker and Berger, 1971; Bé, 1977), and this assures preservation on the flanks of undersea mountains even in the Pacific (e.g. Thompson, 1981). Accordingly, we decided to examine *G. scitula* as a plausible recorder of the chemical environment of sub-intermediate water.

Although carbon and oxygen isotopes from foraminiferal shells are useful tools for reconstructing paleoceanic environments, recent laboratory experiments indicate carbon and oxygen isotopes are affected by other ambient variables. Ortiz et al. (1996) pointed out the temperature and food effects on $\delta^{13}C$ disequilibria in four planktonic species. On the other hand, culture experiments revealed that the carbonate ion concentration in ambient water is also an important factor affecting shell isotopic compositions (Spero et al., 1997). These effects are species specific (Bemis et al., 1998; Bemis et al., 2000). If this is also the case for *G. scitula*, the conventional paleotemperature equations previously proposed (Erez and Luz, 1983; Bouvier-Soumagnac and Duplessy, 1985) could be offset in the carbonate tests of this species. In this study, we examine the effects which alter the isotopic imprint of *G. scitula* collected by the multiple opening/closing net environmental sensing system (MOCNESS) plankton tows and with the sediment traps together with chemical and isotopic properties of the water column.

Of interest is how pore morphology responds to changes in environmental factors. Some shell morphologic parameters (e.g. pore density and porosity) have been investigated on foraminifers to reveal the climatic changes in the past (Bé, 1968; Bé et al., 1973; Hecht et al., 1976). The function of the pores may be related to salinity, temperature and density (Bijma et al., 1990; Frerichs et al., 1972). However, most of these studies were conducted on surface dwelling foraminifers. Since carbonate chemistry in

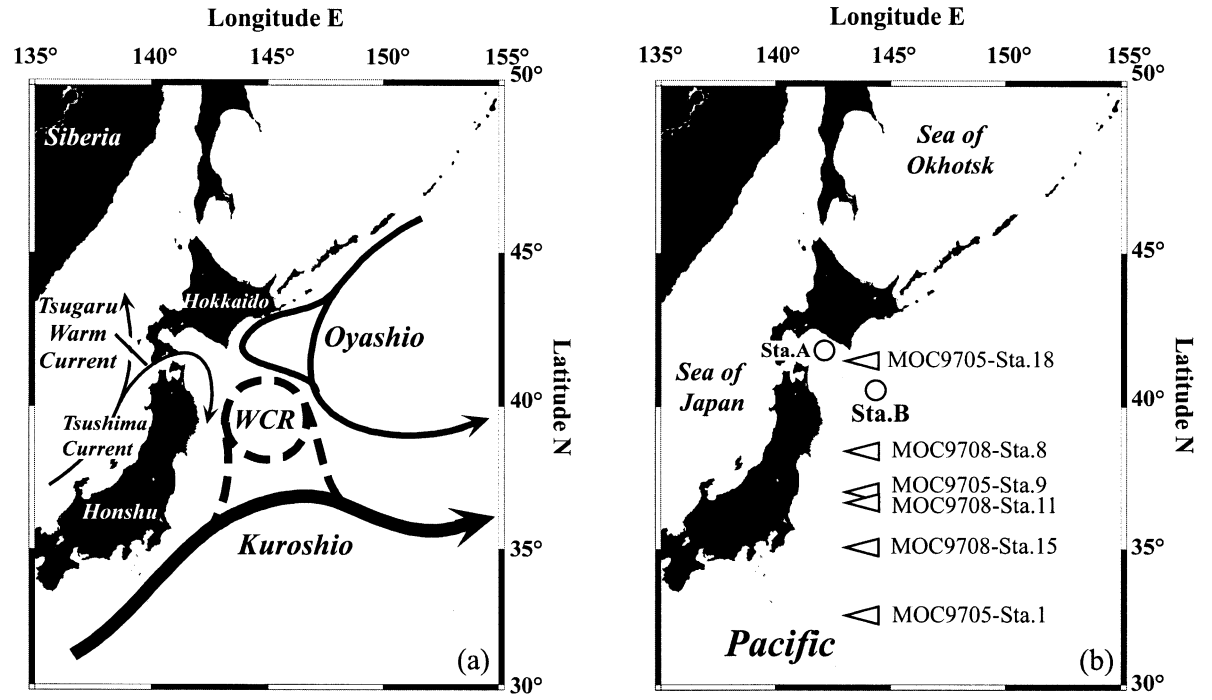

Fig. 1. (a) Surface currents in the NW Pacific, and (b) locations of MOCNESS tows and sediment trap mooring at Sta. B (40°30′N 144°30′E) and at Sta. H (41°30′N 141°30′E) used in this study.

sub-intermediate depths is different from that in surface water, we examine the relation between pore morphology of *Globorotalia scitula* and carbonate chemistry.

In this paper, we evaluate the utility of *Globorotalia scitula* as a proxy for sub-intermediate water depths and use it as a new tool to reconstruct carbonate chemistry by combining isotopic and morphological imprints.

2. Materials and methods

2.1. Experimental design

The study sites lie in a transition zone between less saline, cold Oyashio water to the north, and relatively more saline, warm Kuroshio water to the south (Fig. 1). The Oyashio is the western boundary current of the sub-arctic circulation flowing southward along the Kuril Islands, originating in the high latitudes of the North Pacific. This low-salinity water meets with the Tsugaru warm current (Yasuda et al., 1988) and Kuroshio warm core rings (Yasuda et al., 1992), where they are strongly modified northeast of Honshu Island. This area is refered to as 'the mixed water region (MWR)'. The relative strength of the two water masses determines the water properties in the study area. Because large temporal and spatial variations in hydrography and hydrochemistry can be expected, this oceanic region was selected to evaluate *Globorotalia scitula* as a proxy for changing environments.

2.2. Field methods

2.2.1. MOCNESS sampling

MOCNESS plankton tow samples (Wiebe et al., 1976) were collected during cruises of *R/V Soyo Maru* of National Research Institute of Fisheries Science, Japan along 144E (Fig. 1) in May, August and November 1997 and April 1998. All data reported here were collected during the first two cruises because *Globorotalia scitula* was absent from the

water column during the latter two cruises. Five to seven MOCNESS samples were collected within the depth range from 0 to 800 m at each site using a 64 μm mesh plankton net and were preserved with 10% formalin solution saturated with sodium borate buffer. Because the MOCNESS flow meter did not work properly in May and August 1997, water volumes filtered were estimated using a linear regression method (Ortiz et al., 1995) based on flow meter data during the *Soyo Maru* cruise in April 1998. The standard deviation associated with this calculation is less than 18% (1σ) of the estimated volume filtered.

2.2.2. Sediment trap

Foraminiferal shells were collected by moored sediment traps at two sites, Sta. B located at 40°30′N 144°30′E in about 7500 m water depth from October 1994 to May 1998 and Sta. A located at 41°30′N 142°30′E in about 1200 m water depth from July 1996 to May 1997 (Fig. 1). Each mooring consisted of a cone-shaped HX-10 type sediment trap with 13 time-series collector cups and a baffled collection area of 0.196 m^2 (Noriki et al., 1995). The sediment traps moored at Sta. B and Sta. A were deployed at a water column depth of about 1000 (700–1300) and 600 m, respectively. The sample collection containers of sediment trap were replaced at 14- to 35-day open/close intervals so that we could perform time-series collection of sinking particles in the water column. Each collector cup was filled with filtered seawater mixed with a buffered formalin solution. Because few individuals of *Globorotalia scitula* were collected at Sta. A, shell fluxes are not discussed in this paper, but only their morphotype is shown.

2.2.3. Hydrographic observation

Just after the MOCNESS plankton tows, CTD/Rosette casts were deployed from 0 to 1500 m at each station. Water samples were taken and analyzed for salinity, dissolved oxygen, NO_3^-, total dissolved carbon, total alkalinity, $\delta^{13}C$ of $\sum CO_2$ ($\delta^{13}C_{DIC}$) and $\delta^{18}O$ of H_2O ($\delta^{18}O_w$).

Hydrographic data was collected by the Japan Meteorological Agency (JMA) at both mooring sites (Appendix A). As $\delta^{18}O$ of seawater, $\delta^{13}C$ of $\sum CO_2$, $\sum CO_2$ and total alkalinity were not observed by JMA at the sediment trap mooring site (Sta. B), these are estimated based on the empirical relationship with water temperature, nitrate concentration, apparent oxygen utilization (AOU) and salinity (see Appendix A). To account for the time required for shell production and for settling into sediment, isotope compositions and morphological information of *Globorotalia scitula* are compared with the hydrographic properties observed two weeks before the shell collection.

2.3. Laboratory methods

2.3.1. Foraminiferal sample preparation and isotope analysis

Sediment trap samples were split the fractions into aliquots of 3/10 to 1/2 of the total sample volume before wet sieving. Planktonic foraminifers collected with MOCNESS and sediment trap were concentrated in saturated NaCl solution (Watkins et al., 1996 and were wet sieved by 500, 350, 250 and 210 μm mesh screens, and then dried at 60°C. Due to difficulty in identification among juvenile *menardii*-form globorotaliids, the 210–500 μm size fraction was counted to calculate shell abundance and flux.

Prior to isotopic determination, all foraminiferal shells were roasted in vacuum for 30 min at 375°C. In this study, the isotopic measurements were conducted on one or two individuals (Oba, 1988). Foraminiferal shells were reacted with 100% H_3PO_4 at 60°C and isotope ratios of the evolved CO_2 gas were determined on a Finnigan MAT 251 mass spectrometer with a tepler pumping small inlet system. Isotope compositions are reported in the δ notation as per mil deviations from the international VPDB. A working standard calibrated against NBS-19 (Coplen, 1996) was measured several times in each sample run. External precisions for $\delta^{18}O$ and $\delta^{13}C$ were ± 0.10 and $\pm 0.05‰$, respectively.

2.3.2. Isotope, nutrient and DIC analysis of seawater

Water samples taken during SY9705 and SY9708 were analyzed for oxygen isotope of seawater, carbon isotope of total dissolved carbon $\sum CO_2$, total alkalinity and nutrients.

40 ml of samples for $\delta^{13}C_{DIC}$ was reacted with 95% H_3PO_4 in a vacuum-tight reaction vessel. The evolved CO_2 gas was collected in a liquid nitrogen trap. Then, the water vapor and gases other than CO_2 were removed by vacuum distillation, and the purified CO_2 was sealed in glass tubes. Purified CO_2 was

then analyzed for isotopic composition on a Finnigan MAT deltaS mass spectrometer. Replicate precision of the full procedure is better than ±0.05‰.

The oxygen isotope composition of seawater was determined with CO_2 equilibration with an automated preparation device attached to a Finnigan MAT deltaS. The external reproducibility was ±0.05‰. The analytical results were calibrated against VSMOW and VSLAP standard waters. The $\delta^{18}O_w$ correction of −0.27‰ was applied to convert from VSMOW to VPDB scale.

Total dissolved inorganic carbon (DIC) and total alkalinity measurements were made following the procedures of Ono and Sasaki (2000). The cumulative error in calculated $[CO_3^{2-}]$ is ±5 μmol/kg due to combined measurement errors of two measured parameters. Nutrient samples were analyzed with an autoanalyzer (TRACCS-800). Appendix A describes details for the estimates.

Because the oxygen isotopes of seawater, total inorganic carbon and total alkalinity were not measured by JMA, we estimated these with temperature, salinity, AOU and nitrate by using multiple regression analysis (see Appendix A).

2.4. Morphometrics

SEM investigations were performed on an HITACHI S-3200N scanning electron micrograph at 20 kV. Each specimen was placed on a stage with double-sided plastic tape. Preparation without ion spattering operation makes subsequent isotopic analysis possible. Photographs were processed with an HITACHI EP-3100L Image Processor and converted to digitized files. We focused on the spiral side of the last two chambers in 250–350 and 350–500 μm size fraction in the study. Isotopic analysis of the samples followed the SEM observations. From MOCNESS and sediment trap samples, 22 and 26 individuals were measured. All samples collected by sediment traps within each collection period were averaged. Morphological data for MOCNESS samples collected in the same tows were also averaged.

Pore density is based on the averaged number of pores in an area of 25×25 μm^2. Mean porosity of the shell wall was calculated in terms of percentage of open pore area per unit shell area. Pore area was determined on the outer test surface. To improve measured precision, this procedure was repeated for at least three different positions and was continued until a minimum of 50 pores were counted for each chamber.

3. Oceanography at sediment trap mooring site (Sta. B)

The seasonal pattern of hydrography at Sta. B was primarily associated with replacements of water masses, the Oyashio Water and the Kuroshio warm-core ring water. Winter deep convection was more pronounced when the warm core rings were distributed (Fig. 2). The less saline Oyashio flowed into the mooring site in spring and was modified due to summer insolation, and then the seasonal thermocline developed (Fig. 2).

4. Sediment trap results

The *Globorotalia scitula* shell flux pattern was documented from 1994–1998 (Fig. 3a). Because the sediment trap container did not rotate between December 1996 and May 1997, the mean shell flux for the entire period is shown. The high shell fluxes were found during winter and early spring months and reached a maximum shell flux of 61 shells/m^2/day from 13 December 1995 to 10 January 1996. By contrast, there was little shell flux in summer. Seasonal successions of *G. scitula* shell fluxes at Sta. B were in good agreement with that observed in the eastern Pacific transition zone (Ortiz and Mix, 1992). Therefore, *G. scitula* may flourish mainly during winter in the temperate North Pacific.

5. MOCNESS results

5.1. Standing stock

The standing stock of *Globorotalia scitula* and estimates of water volume filtered are listed in Table 1. Table 2 contains the calculated mean values of $\delta^{13}C$ of $\sum CO_2$ ($\delta^{13}C_{DIC}$), $\delta^{18}O_w$, $[CO_3^{2-}]$, and calcite saturation state ($\Omega_{calcite}$, see Appendix B for details) for each MOCNESS plankton tow depth range. *G. scitula* was found at the water depths close to saturation horizon

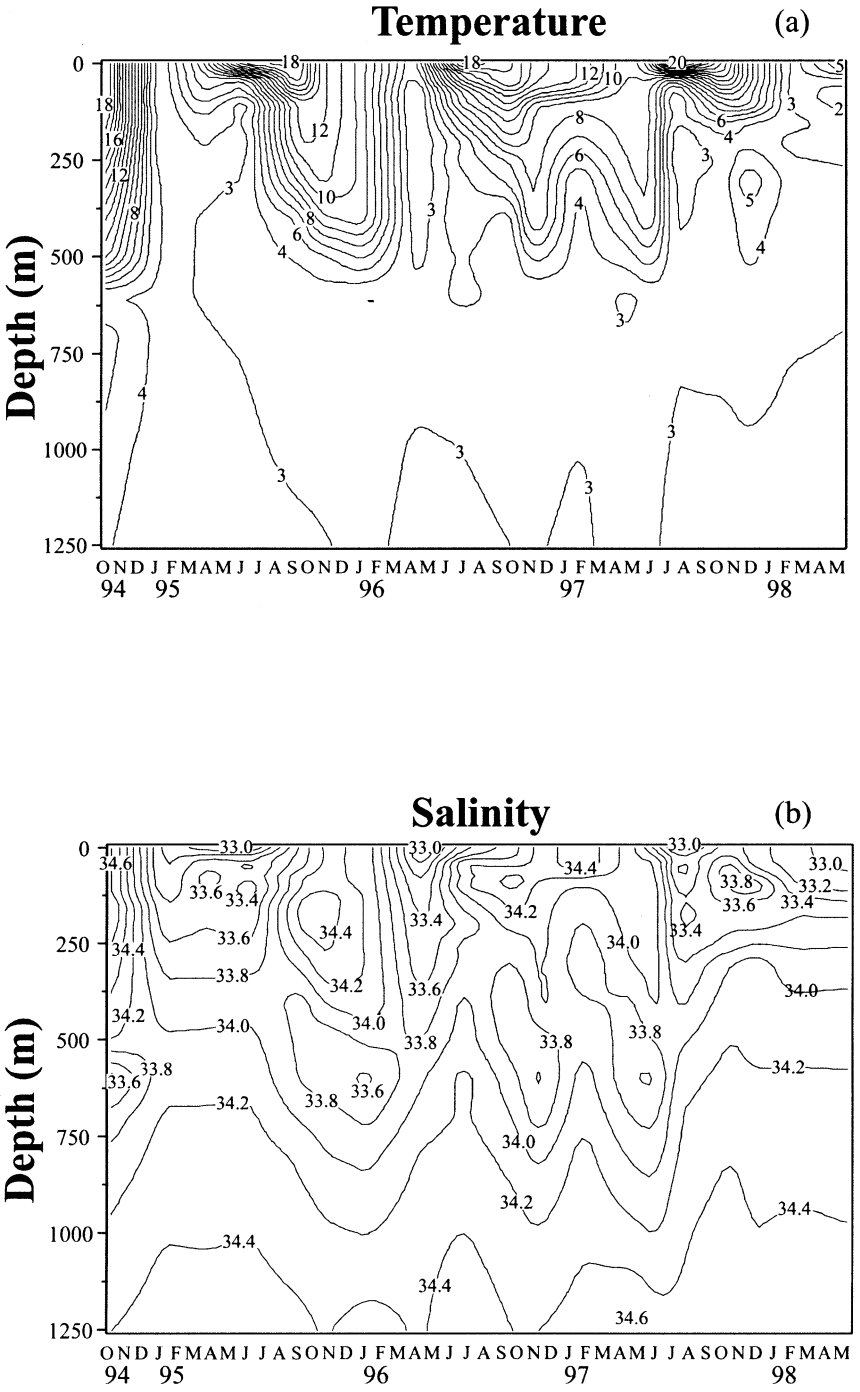

Fig. 2. Temporal variation of (a) temperature, and (b) salinity at Sta. B.

Table 1
The standing stock and environmental variables at MOCNESS tow stations during *R/V Soyo Maru* 9705 and 9708 cruises. Size fraction of 210–500 μm were counted

Date	Tow site		MOC station No.	Local time	Depth range (m)	Mean temp. (°C)	Mean salinity	Mean σ_θ	Number of specimens	Volume[a] filtered (m^3)	Standing stock ($\#/10^{-3}m^3$)
	Lat. N	Long. E									
5/15/97	41°31′	144°03′	MOC	3:24	130–180	4.2	33.46	26.55	0	99	
			9705	↓	180–230	3.9	33.48	26.59	0	124	
			Sta.18	5:22	230–280	3.9	33.54	26.64	0	139	
					280–380	2.8	33.48	26.69	1 ± 1	173	6
					380–470	2.4	33.56	26.78	0	257	
					470–580	2.8	33.72	26.89	0	232	
5/12/97	37°00′	143°57′	MOC	5:24	180–270	10.4	34.33	26.37	0	139	
			9705	↓	270–380	8.7	34.29	26.61	0	155	
			Sta.9	7:12	380–480	7.1	34.25	26.81	0	212	
					480–560	5.6	34.26	27.01	0	132	
					560–580	5.1	34.27	27.09	3 ± 2	127	24
					580–680	4.5	34.28	27.16	0	190	
					680–800	3.8	34.30	27.25	0	215	
5/11/97	33°01′	144°02′	MOC	5:35	100–180	18.0	34.81	25.14	0	49	
			9705	↓	180–270	17.4	34.81	25.28	0	88	
			Sta.1	6:45	270–380	14.7	34.60	25.74	0	133	
					380–480	11.5	34.37	26.21	0	216	
					480–580	9.0	34.24	26.53	0	185	
					580–680	7.0	34.19	26.79	1 ± 1	475	5
					680–720	5.7	34.19	26.96	1 ± 1	131	8
8/24/97	38°32′	143°59′	MOC	19:08	30–170	13.9	34.33	25.69	0	147	
			9708	↓	170–330	8.6	34.15	26.52	0	168	
			Sta.8	20:54	330–430	4.8	33.76	26.71	0	102	
					430–630	4.5	33.99	26.93	5 ± 2	301	17
					630–810	3.7	34.18	27.17	7 ± 3	367	19
8/25/97	37°00′	143°55′	MOC	16:18	20–170	12.0	34.43	26.15	0	132	
			9708	↓	170–320	6.9	34.09	26.72	0	148	
			Sta.11	18:08	320–420	5.4	34.18	26.97	2 ± 1	127	16
					420–620	4.2	34.18	27.10	7 ± 3	297	24
					620–810	3.2	34.26	27.27	4 ± 2	346	12
8/26/97	35°03′	143°57′	MOC	10:35	20–160	15.2	34.50	25.54	0	138	
			9708	↓	160–320	9.3	34.20	26.44	0	165	
			Sta.15	12:30	320–410	7.2	34.16	26.73	0	142	
					410–620	5.2	34.20	27.02	0	376	
					620–690	4.4	34.26	27.16	4 ± 2	305	13

[a] Volume filtered was estimated using the following relationship: $V_f = 14.7(t) + 14.3$ ($r^2 = 0.95, n = 64, p < 0.001$). V_f and t represent water volume filtered in 10^3 cubic meters and the tow duration in minutes, respectively.

with respect to calcite (Table 2). As all individuals contained protoplasm, we infer that samples were not collected long after death. Hence, *G. scitula* was inhabiting the depths where they were collected, even though surrounding seawater was barely saturated with respect to calcite. Meanwhile, at depths shallower than 300 m, no *G. scitula* were found in the MOCNESS tow site. *G. scitula* was observed within the water density interval between 26.7 and 27.3σ_θ in both daytime and night time MOCNESS samples. The maximum abundance of 48 shells/10^3/m^3 was observed around the 27.1 σ_θ

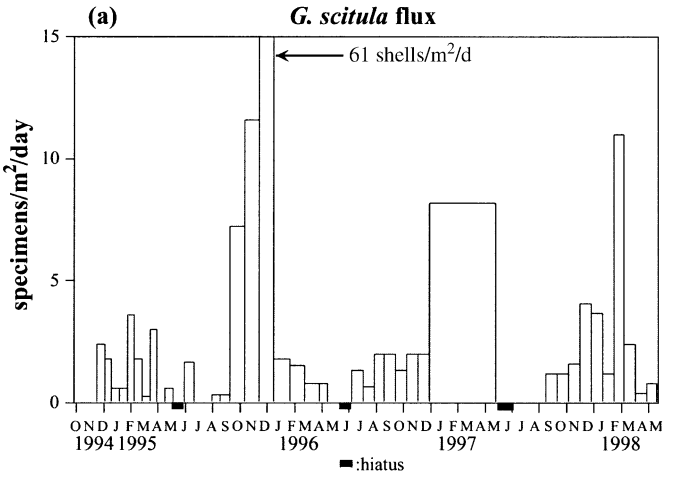
(a)
G. scitula flux
61 shells/m2/d
specimens/m2/day
15
10
5
0
O N D J F M A M J J A S O N D J F M A M J J A S O N D J F M A M J J A S O N D J F M A M
1994 1995 1996 1997 1998
:hiatus

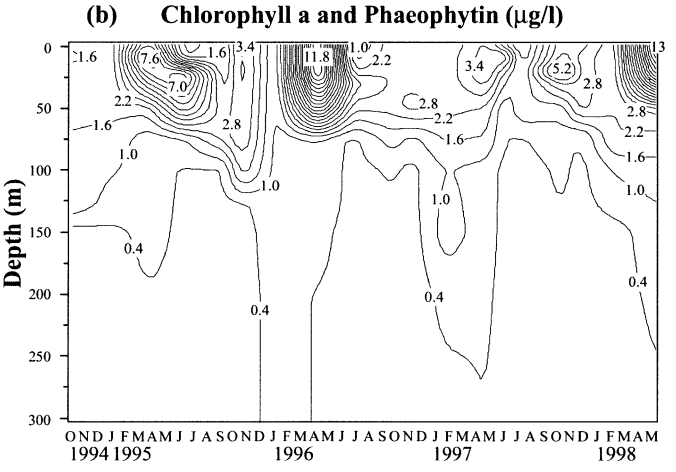
(b)
Chlorophyll a and Phaeophytin (μg/l)
Depth (m)
0
50
100
150
200
250
300
1.6
7.6
7.0
1.6
3.4
11.8
1.0
2.2
3.4
5.2
2.8
2.2
2.8
1.6
2.8
2.2
2.8
1.6
1.0
1.0
1.0
1.0
1.6
1.0
0.4
0.4
0.4
0.4
O N D J F M A M J J A S O N D J F M A M J J A S O N D J F M A M J J A S O N D J F M A M
1994 1995 1996 1997 1998

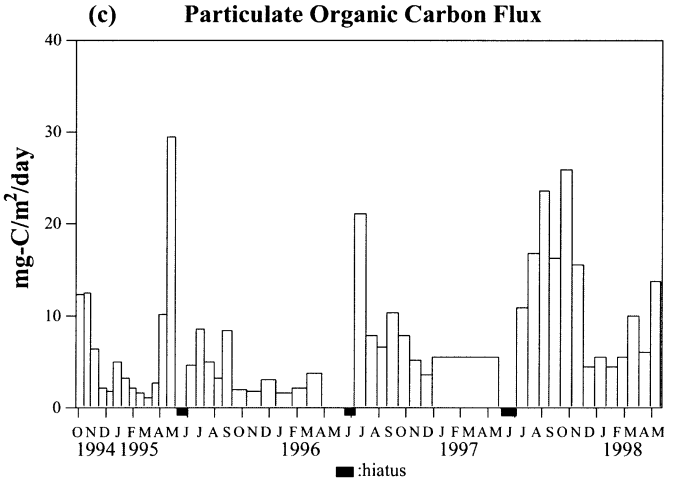
(c)
Particulate Organic Carbon Flux
mg-C/m2/day
40
30
20
10
0
O N D J F M A M J J A S O N D J F M A M J J A S O N D J F M A M J J A S O N D J F M A M
1994 1995 1996 1997 1998
:hiatus

Table 2
Temperature, salinity, carbonate ion concentration, $\delta^{18}O$ of seawater, $\delta^{13}C$ of ΣCO_2 and isotopic compositions of *Globorotalia scitula*. In case of replicated analysis of foraminiferal sample at a single depth range, we reported the mean value +/− standard error of mean. Data for 35°N 144°E during SY9708 cruise is not included because total dissolved inorganic carbon and total alkalinity were not measured

MOC station	Depth (m)	Size fraction (μm)	$\delta^{13}C_{G.scitula}$ (‰ PDB)	$\delta^{18}O_{G.scitula}$ (‰ PDB)	Mean temp. (°C)	Mean salinity	Mean σ_θ	Mean $\delta^{13}C_{DIC}$ (‰ PDB)	Mean $\delta^{18}O_w$ (‰PDB)	Mean $[CO_3^{2-}]$ (μmol/kg)	Mean Ω_{cal}[a]
9705 Sta.1	570–680	250–350	−0.27	1.03	7.0	34.2	26.8	−0.09	−0.40	58	1.2
	680–720	210–250	−0.14	1.00	5.7	34.2	27.0	−0.34	−0.48	54	1.0
9705 Sta.9	560–580	250–350	0.13	0.23	5.1	34.3	27.1	−0.29	−0.45	69	1.4
			0.33	0.78							
		210–250	0.41	1.47							
9705 Sta.18	280–380	250–350	−0.41	0.80	2.8	33.5	26.7	0.27	−0.79	83	1.7
9708 Sta.8	420–630	350–500	0.31	1.32	4.5	34.0	26.9	−0.06	−0.53	59	1.2
		210–250	0.27	1.66							
	630–810	250–350	−0.06	1.70	3.9	34.2	27.2	−0.33	−0.49	59	1.1
			0.28	1.44							
			−0.09	1.74							
		210–250	0.06	1.35							
9708 Sta.11	320–420	250–350	−0.32	0.41	5.4	34.2	27.0	−0.10	−0.44	74	1.5
	420–620	250–350	0.08	1.36	4.2	34.2	27.1	−0.39	−0.51	58	1.2
			0.03	1.38							
			−0.19	0.86							
			−0.35	0.79							
			0.14	1.30							
	620–810	350–500	0.89	1.32	3.2	34.3	27.3	−0.53	−0.52	54	1.0
		250–350	0.36	2.00							
		210–250	0.04	1.78							

[a] Ω_{cal} represents the calcite saturation state. See Appendix B.

isopycnal (Fig. 4 and Table 1). In the corresponding isopycnal layers, temperature and salinity ranged 3–7°C and 33.5–34.3 psu, respectively. The observed temperature range is also within the value reported by Bé and Tolderlund (1971).

5.2. Stable isotopes

The mean $\delta^{18}O_{G.\ scitula}$ was 1.23 ± 0.46‰ (n = 21). Mean temperature within each MOCNESS towing depth is plotted against the $\Delta\delta^{18}O_{G.\ scitula} = \delta_{18}O_{G.\ scitula} - \delta^{18}O_w$ (Fig. 5). Hereafter, the isotopic values from the 250–500 μm size fraction were used for statistics to avoid size effect. Assuming the linear relation between $\Delta\delta^{18}O_{G.\ scitula}$ and temperature (t), the following relation can be found:

$$\Delta\delta^{18}O_{G.\ scitula}(= \Delta\delta^{18}O_{G.\ scitula} - \delta^{18}O_w) = -0.280\ (\pm 0.224)t + 2.87(\pm 0.994), \quad (1)$$

$$r^2 = 0.33, \qquad n = 16, \qquad p < 0.05.$$

Quoted errors on the slope and intercept are 95%

Fig. 3. (a) *Globorotalia scitula* shell flux at Sta. B for 210–500 μm size fraction. (b) Temporal variation in the chlorophyll-*a* and phaeophytin concentration (μg/l) in the upper 300 m at Sta. B. Note the difference in vertical scale from Figs. 2 and 8. (c) Particulate organic carbon flux at Sta. B. POC contents for samples observed from July 1996 to May 1998 were indirectly calculated by using the equation proposed by Noriki et al. (1990).

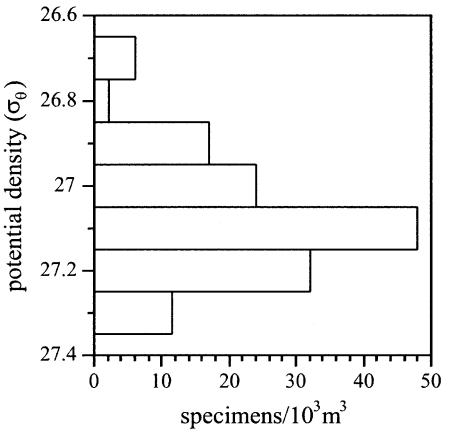

Fig. 4. Histogram of standing stock of *G. scitula* plotted against water density in σ-notation. All data collected during MOCNESS towing are tallied together.

confidence limits. $\Delta\delta^{18}O_{G.\ scitula}$–$t$ relationship predict lower temperatures relative to the paleotemperature equation for *G. menardii* generated with field experiment, which is compared in Fig. 5 (Bouvier-Soumagnac and Duplessy, 1985; $\delta^{18}O_{G.\ menardii} - \delta^{18}O_w = -0.199t + 2.903$). As $\Delta\delta^{18}O_{G.\ scitula}$–$t$ relationship is not significant, the $\Delta\delta^{18}O_{G.\ scitula}$ may not depend only on temperature (Fig. 5). Since the $\delta^{18}O$ of foraminiferal shells may not be controlled solely by temperature, but also by the carbonate ion concentration in ambient water (Spero et al., 1997), we suggest that a CO_3^{2-} concentration term should be introduced into the above equation.

The mean $\delta^{13}C_{G.\ scitula}$ and $\delta^{13}C_{DIC}$ was $0.07 \pm 0.31‰$ (1σ) and $-0.28 \pm 0.19‰$ (1σ) for the MOCNESS towing depths, respectively (Table 2). Romanek et al. (1992) demonstrated that calcite in equilibrium with DIC ($\delta^{13}C_{eq}$) should be enriched by 1‰ relative to $\delta^{13}C_{DIC}$. Carbon isotopic compositions in *Globorotalia scitula* were offset from calculated $\delta^{13}C_{eq}$ at most depths, and the offset from the equilibrium was larger at shallower depths (Table 2).

6. Pore morphology of *Globorotalia scitula*

Pore size was highly variable in the samples collected in the MOCNESS tows (Plate 1a–c) and in the sediment trap (Plate 1d–f). Shell porosity on *Globorotalia scitula* ranged 8–35% (Table 3). In

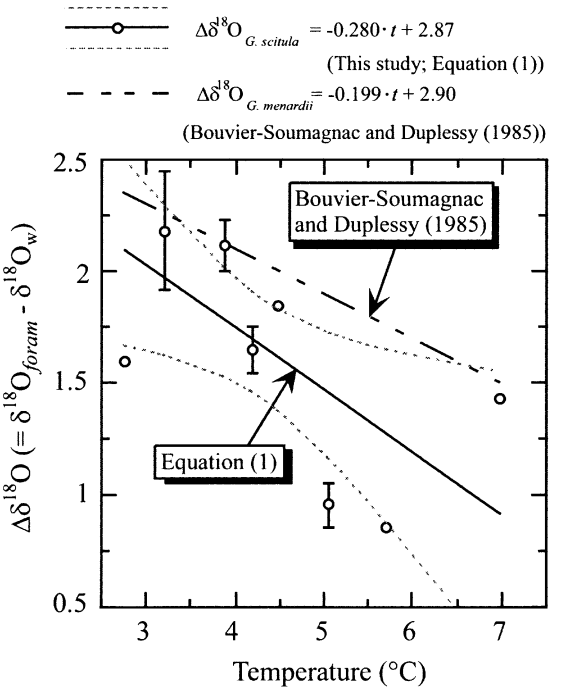

Fig. 5. $\Delta\delta^{18}O(= \delta^{18}O_{G.\ scitula} - \delta^{18}O_w)$ values (‰ VPDB scale) vs. temperature for MOCNESS samples (250–500 μm fraction; open circle). Mean temperature and $\delta^{18}O_w$ for each collection depth range are used. The observed $\Delta\delta^{18}O_{G.\ scitula}$:$t$ relationship (Eq. (1); open circle) is plotted. Dotted lines represent 95% interval estimate for Eq. (1). Error bars represent ± standard error of the mean. The $\Delta\delta^{18}O$:t relationship for *G. menardii* (broken line) is presented for reference (Bouvier-Soumagnac and Duplessy, 1985).

contrast to other *Globorotalia* (Bé, 1968), the funnel-shaped cross section of pores was identified in penultimate and antepenultimate chambers, though most of pores in ultimate chamber are cylindrical shaped (Plate 1). Interestingly, large pore area can be seen in penultimate and antepenultimate chambers rather than in the ultimate chamber (Plate 1). In addition, pore density decreased with increasing porosity and pore diameter (Table 3).

7. Discussions

7.1. Relation between Globorotalia scitula flux and environmental variables

In order to use *Globorotalia scitula* as a paleoceanographic tool, we must know at which time of year

Table 3
Shell porosity and environmental variables at the habitat depth. When more than one sample was measured morphometrically, we report the mean value +/− standard error of the mean

	Station	Latitude N	Longitude E	Water Mass[a]	No. of sample	$\delta^{18}O_{G.\ scitula}$[b] (‰)	Depth (m)	Temp. (°C)	Salinity	σ_θ	CO_3^{2-} (μmol/kg)	$\Omega_{calcite}$	Pore diameter (μm)	Pore density	Porosity (%)
MOC	9705-Sta.1	33°01′	144°02′	Kuroshio	1	1.03	570–680	7.0	34.19	26.8	58	1.2	3.7	5.7	10
MOC	9705-Sta.9	37°00′	143°57′	MWR	2	0.51	560–580	5.1	34.27	27.1	69	1.4	4.5 ± 1.1	4.9 ± 1.2	11 ± 3
MOC	9705-Sta.18	41°31′	144°03′	Oyashio	1	0.80	280–380	2.8	33.48	26.7	83	1.7	3.4	4.9	7
MOC	9708-Sta.8	38°32′	143°59′	MWR	1	1.32	420–630	4.5	33.98	26.9	59	1.2	6.5	2.8	15
MOC	9708-Sta.8	38°32′	143°59′	MWR	3	1.63	630–810	3.9	34.20	27.2	59	1.1	6.1 ± 0.3	3.8 ± 0.1	18 ± 2
MOC	9708-Sta.11	37°00′	143°55′	MWR	1	0.41	320–420	5.4	34.18	27.0	74	1.5	3.0	5.7 0.0	7
MOC	9708-Sta.11	37°00′	143°55′	MWR	5	1.14	420–620	4.2	34.18	27.1	58	1.2	5.1 ± 0.8	4.2 ± 0.3	14 ± 3
MOC	9708-Sta.11	37°00′	143°55′	MWR	2	1.66	620–810	3.2	34.26	27.3	54	1.1	5.7 ± 0.4	3.9 ± 0.2	17 ± 4
Average								4.5	34.1	27.0	67	1.3	4.8	4.5	12

	Station	Collection Period	Water Mass[a]		$\delta^{18}O_{G.\ scitula}$ (‰)	Predicted depth (m)[c]	Temp. (°C)	Salinity	σ_θ	CO_3^{2-}[d] (μmol/kg)	$\Omega_{calcite}$[d]	Pore diameter (μm)	Pore density	Porosity (%)
Sed Trap	Sta. B	2/16/95–03/05/95	Oyashio	4	1.33	205	2.0	33.5	26.8	61	1.2	7.8 ± 1.6	4.0 ± 1.0	24 ± 2
Sed Trap	Sta. B	10/05/95–11/06/95	MWR	8	1.24	690	3.8	34.0	27.0	66	1.3	7.7 ± 0.9	2.9 ± 0.3	20 ± 3
Sed Trap	Sta. B	12/10/95–01/13/96	MWR	4	1.46	668	3.6	33.8	26.9	59	1.2	7.2 ± 1.4	3.6 ± 0.6	23 ± 6
Sed Trap	Sta. B	08/24/97–09/18/97	Oyashio	2	2.12	848	2.8	34.2	27.2	50	0.9	8.1 ± 2.0	3.4 ± 0.5	28 ± 10
Sed Trap	Sta. B	10/13/97–11/07/97	MWR	1	2.11	598	3.3	34.3	27.3	44	0.9	9.2	2.6	28
Sed Trap	Sta. B	11/07/97–12/02/97	MWR	1	2.19	697	3.2	34.3	27.3	44	0.9	6.6	5.0	27
Sed Trap	Sta. B	12/02/97–12/27/97	MWR	3	2.18	884	3.1	34.4	27.4	47	0.9	9.5 ± 1.5	3.2 ± 0.5	35 ± 4
Sed Trap	Sta. B	02/15/98–03/12/98	Oyashio	3	2.01	344	3.5	34.0	27.0	42	0.9	6.8 ± 1.7	4.1 ± 1.0	23 ± 9
Average							3.2	34.1	27.1	51	1.0	7.9	3.6	26

[a] Water masses are divided into the Kuroshio, the Mixed Water Region (MWR) and the Oyashio.
[b] Shell size of 250–500 μm were measured.
[c] The habitat depth of sediment trap samples were predicted with Equation (4) (See text).
[d] Carbonate ion concentration and calcite saturation state (Ω_{cal}) at Sta. B were estimated using multiple regression analysis as described in Appendix A.

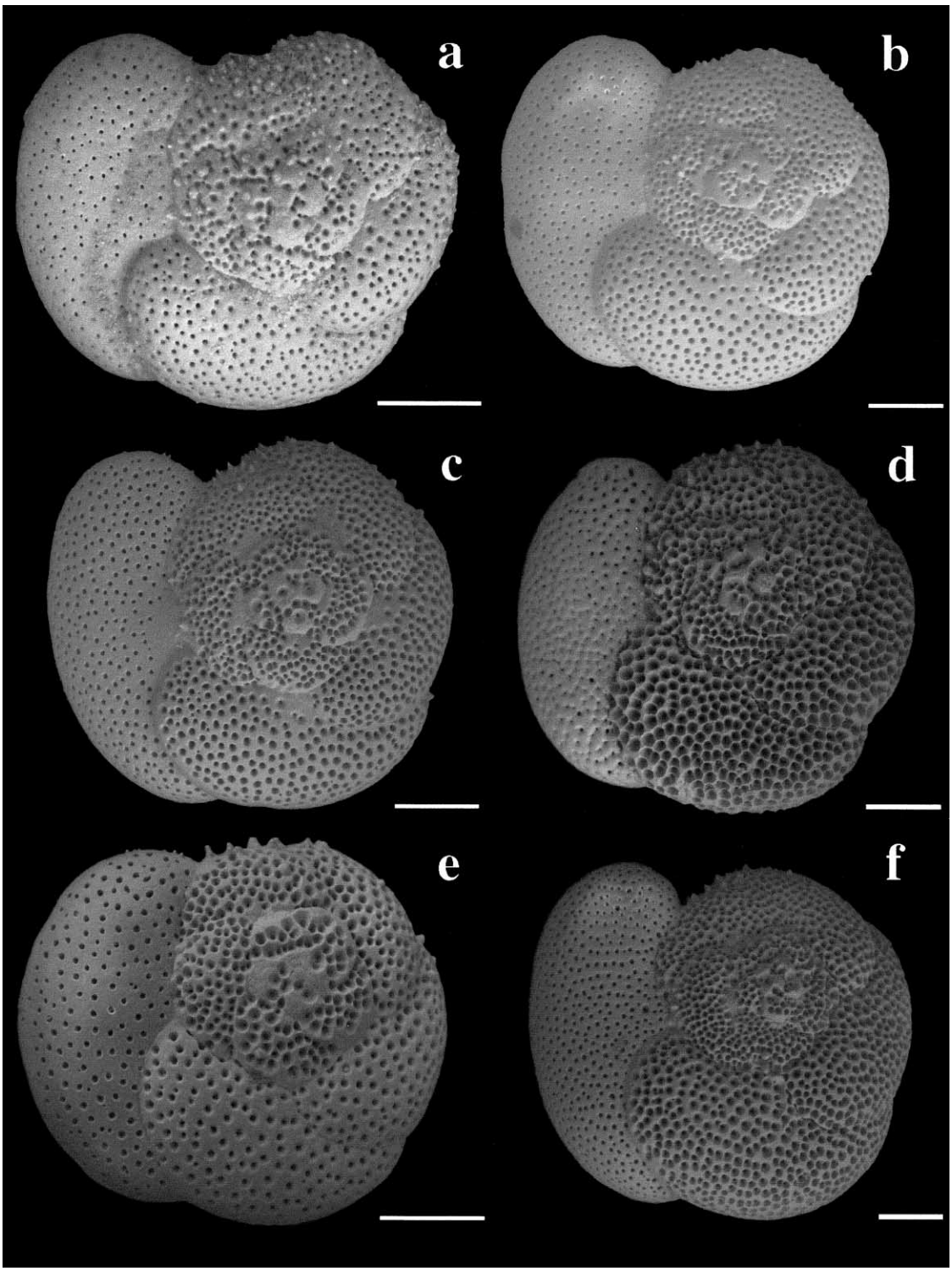
a
b
c
d
e
f

G. scitula calcified their shells and the relation between *G. scitula* flux and environmental variables. Deep-living globorotaliids, e.g. *G. hirsuta*, are considered to consume particulate organic matter, so-called marine snow (Hemleben et al. 1989). Whereas the shell flux increased from winter to early spring, POC flux was considerably lower at that time (Fig. 3a and c). Thus, the amount of particulate organic matter, which has a high settling velocity, was not responsible for the presence of *G. scitula*.

Surface dwelling planktonic foraminifers secrete their shells mainly in the chlorophyll-*a* maximum zone (Fairbanks and Wiebe, 1980). Is this the case for *Globorotalia scitula*? The peak shell fluxes coincided with the appearance of warm core rings (Figs. 2 and 3a). This trend was pronounced during winter in 1995–96 and 1996–97. Within the warm core rings, deeply distributed pigments (chlorophyll-*a* and phaeophytin) were found; however, the timing was not entirely in accordance with increase in *G. scitula* shell fluxes (Figs. 2 and 3a). An increase in standing stock of planktonic foraminiferal assemblages corresponds to intensified surface layer mixing due to storms (Schiebel et al., 1995). Thus, the fluctuation in the standing stock of *G. scitula* in the upper export zone (above 700 m water depth) may have corresponded with the wind velocity. Extensively decomposed suspended POC is distributed evenly in the warm core ring (Saino, 1992). The non-spinose species (e.g. *G. hirsuta*) do not accept living prey because of their rhizopodial net is incapable of holding them (Hemleben et al., 1989). Thus, *G. scitula* may prefer fine, suspended POC, even if it is not newly produced POC. The abundance of *G. scitula* in sediment, therefore, would basically correspond to intensified vertical mixing.

7.2. Implication of pore morphological variability

High porosity was clearly seen on each chamber except the final chamber, especially on specimens collected with sediment trap at Sta. A (Plate 1d). The final chamber of this individual is relatively new because more than a half of pores on the final chamber do not yet penetrate the wall. As proposed by Hemleben et al. (1977) since no other calcification occurs on the surface of the penultimate chamber during the early stage of final chamber formation, pores on older chambers become enlarged before the final chamber formation. These facts imply that the difference in porosity between final and penultimate chambers is not caused by dissolution after death. Accordingly, we discuss the relation between environmental variables and porosity on penultimate chambers. In this paper, the relations of shell porosity to salinity and calcite saturation state ($\Omega_{\mathrm{calcite}}$; see Appendix B) were examined.

Baumfalk et al. (1987) found high pore density on *Globorotalia scitula* recovered from sapropel layers in the Mediterranean and proposed that low salinity was a driving mechanism behind the increase in pore density. Indeed, *G. scitula* collected from the recent North Pacific has high porosity or pore density (Reynolds and Thunell, 1985; Thunell and Reynolds, 1984). In contrast, recent *G. scitula* collected from the Mediterranean Sea have fewer pores (Thunell, 1978; Plate II therein). Thus, the low salinity hypothesis might be plausible. However, we could not confirm the relationship between shell porosity or pore density to salinity in our study area (Table 3). Less saline water was probably distributed in the Mediterranean when sapropel layers were formed, although the contemporaneously developed surface stratified layer (e.g. Jorissen, 1999) could also have lowered pH at the sub-intermediate depths. By contrast, the upper part of water column in the present Mediterranean Sea is supersaturated enough to prevent *G. scitula* from dissolution. Accordingly, we speculate these differences in shell porosity could be caused by change in calcite saturation state of ambient water.

The inverse covariation between porosity and calcite saturation state ($\Omega_{\mathrm{calcite}}$) is evident (Fig. 6). Shell porosity of MOCNESS samples increase from 8 to 18% with decreasing calcite saturation state from 1.7 to 1.1. By morphological investigations, Troy et al. (1997) confirmed a remarkable dissolution of

Plate 1. *Globorotalia scitula* SEM images from (a– c) MOCNESS samples and (e–g) sediment trap samples. Scale bars indicate 100 μm. (a) SY9705 Sta.18, 280–380 m, 250–350 μm, (b) SY9708 Sta. 8, 630–810 m, 350–500 μm, (c) SY9708 Sta. 8, 630–810 m, 250–350 μm, (d) Sta. A, 12/27/96–1/21/97, 350–500 μm, (e) Sta. B, 12/10/95 ∽ 1/13/96, 350–500 μm, and (f) Sta. B, 12/2/97–12/27/97, 350–500 μm.

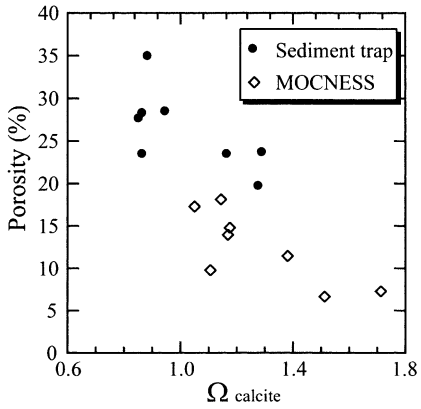

Fig. 6. Shell porosity plotted against the calcite saturation state (Ω_{cal}). All pore morphometrics are conducted on penultimate chamber (spiral side).

carbonate mineral, which were deployed in the intermediate depth for three days in the tropical Pacific, by using atomic force microscopy (AFM). Calcite minerals deployed at intermediate water depths (i.e. 500–1000 m) in which $\Omega_{calcite}$ is approximately unity showed the rough surface morphology indicating dissolution. This depth range corresponds to the isopycnal layers where *Globorotalia scitula* dwells. Would dissolution occur on living foraminiferal shells even if most of the foraminiferal shells are coated by organic membrane? Organic coatings may not be important in protecting foraminiferal tests compared to cocoliths (e.g. Morse, 1974). Also, some surface areas have no organic layer on the shells of *G. menardii* collected from plankton tows in the upper 200 m water (Hemleben et al., 1977). Hemleben et al. (1977) also showed the coarsely crystalline shell surface on which organic membrane is absent. We speculate that a lack of organic membrane due to bacterial decomposition could promote dissolution of foraminiferal tests as a result of production of organic acids. In addition, the observed differences in porosity among chambers might reflect the difference in the extent of decomposition of organic membrane (Plate I). Therefore we propose the dissolution hypothesis to explain the increments of porosity on *G. scitula* shells.

7.3. What is the cause of isotopic disequilibria in *Globorotalia scitula*?

A temperature effect on the carbon isotope disequilibria has been proposed (Ortiz et al., 1996); however, the offset between $\delta^{13}C_{G.\ scitula}$ and $\delta^{13}C_{DIC}$ was not related to temperature ($r^2 = 0.09$, $n = 16$). Therefore, we exclude a temperature effect as a major factor governing the carbon isotope disequilibrium for *Globorotalia scitula*. Food concentration may also affect the $\Delta\delta^{13}C_{e-s}(=\delta^{13}C_{eq}-\delta^{13}C_{shell}=(\delta^{13}C_{DIC}+1‰)-\delta^{13}C_{shell})$ of planktonic foraminifera (Ortiz et al., 1996). As discussed above, suspended POC are possible food source for *G. scitula*. Saino (1992) measured suspended POC concentration around our study area, and the POC concentration ranged from 1 to 2 μg/l. The $\Delta\delta^{13}C_{e-s}$ is not sensitive to this order of change in food concentration if the results of Ortiz et al. (1996) are employed. Therefore, food concentration may not have a significant effect on carbon isotopic disequilibrium in *G. scitula*.

As several researchers pointed out, incorporation of respired CO_2, which has significantly lower carbon isotope composition (ca. −20‰), could explain some of the carbon isotopic discrimination in *Globorotalia scitula* shells (Mulitza et al., 1999; Spero and Lea, 1996). In general, the chambers that formed during early growth stages would be isotopically depleted in $\delta^{13}C$ because a relatively large amount of metabolic CO_2 is incorporated into their carbonate shells during the juvenile stage as compared with mature foraminifera (e.g. Hemleben and Bijma, 1994; Kahn and Williams, 1981). Indeed, individuals of amputated *G. scitula* (ultimate, penultimate and remnant chambers of 28 specimens from 250–350 μm size fraction) collected from the sediment traps, showed that the $\delta^{13}C$ and $\delta^{18}O$ in the remnant chambers (−0.41 and +1.28‰) were more depleted than values of the last two chambers (+0.17 and +1.61‰), respectively. This result suggests that respired light carbon is incorporated into small chambers secreted during the juvenile stage. However, as specimens smaller than 210 μm were not used in multiple regression analysis, the respiration effect on isotopic disequilibria can be regarded as small.

Next, we evaluate the effect of $[CO_3^{2-}]$ on isotope compositions on *Globorotalia scitula*. As the $[CO_3^{2-}]$ effect on isotope compositions of planktonic foraminifers is species specific (Bijma et al. 1998; Russell and Spero, 2000), we evaluate the effect of $[CO_3^{2-}]$ on *G. scitula* shells. By incorporating a $k_1[CO_3^{2-}]$ term (k_1 is

constant) into Eq. (1), the following equation is obtained by a multiple regression:

$$\Delta\delta^{18}O_{G.\ scitula} = -0.261(\pm0.177)t - 0.034(\pm0.023) \times [CO_3^{2-}] + 4.64(\pm1.58), \quad (2)$$

$$n = 16, \qquad r^2 = 0.62, \qquad p < 0.01.$$

Quoted errors on the slope and intercept are 95% confidence intervals. The fit of the equation to observed data becomes remarkably improved. Also, regardless of the strong correlation between temperature and $[CO_3^{2-}]$ in seawater, both coefficients are significant ($p < 0.01$). On the other hand, the $[CO_3^{2-}]$ effect on $\Delta\delta^{13}C_{G.\ scitula}$ is given as

$$\Delta\delta^{13}C_{G.\ scitula}(= \delta^{13}C_{G.\ scitula} - \delta^{13}C_{DIC}) = -0.040(\pm0.026)[CO_3^{2-}] + 2.79(\pm1.65), \quad (3)$$

$$n = 16, \qquad r^2 = 0.42, \qquad p < 0.01.$$

Despite the narrow range in $[CO_3^{2-}]$ and the large error, we confirmed that slopes are not significantly different from zero, and negative slopes commonly found in both $\Delta\delta^{18}O_{G.\ scitula}/[CO_3^{2-}]$ and $\Delta\delta^{13}C_{G.\ scitula}/[CO_3^{2-}]$ indicate that the carbonate ion concentration influence isotope composition of *Globorotalia scitula* during chamber formation. However, the apparent $[CO_3^{2-}]$ dependence found in both $\Delta\delta^{18}O_{G.\ scitula}$ and $\Delta\delta^{13}C_{G.\ scitula}$ are too large compared with those for other planktonic foraminifera though a direct comparison with laboratory experiments in which isotopic compositions of each chamber position were separately determined (e.g. Spero et al., 1997) may not be appropriate. If obtained $\Delta\delta^{18}O_{G.\ scitula}/[CO_3^{2-}]$ and $\Delta\delta^{13}C_{G.\ scitula}/[CO_3^{2-}]$ result from contributions of other environmental factors, though the error involved in Eqs. (4) and (5) are large, other possibilities should be examined to interpret those apparent $[CO_3^{2-}]$ effect on *G. scitula*. We speculate that the dissolution effect can potentially be an explanation for relatively strong $[CO_3^{2-}]$ dependence for *G. scitula*. Berger and Killingley (1977) suggested that in *P. obliquiloculata*, from sediment core samples, they interpreted that the dissolution of inner wall, which is secreted during early growth stages and contains low $\delta^{13}C$, increases the $\delta^{13}C$ of remainder. A similar mechanism could exist in *G. scitula*. Since the earlier secreted chambers of *G. scitula* have lower isotopic values than the later chambers, the preferential reduction of the younger chambers through pore enlargement increases the isotopic value of *G. scitula* shells as a whole. In other words, the influence of respired CO_2 on shell isotopic compositions of *G. scitula* could be lessened by preferential reduction of the earliest chambers secreted while in the juvenile stage.

To accommodate the dissolution component, we suggest inserting a calcite saturation term ($\Omega_{calcite}$) into the paleotemperature equation for *Globorotalia scitula*. By inserting a $k_2(1 - \Omega_{calcite})$ term (k_2 is constant) into Eq. (1), we obtain by multiple regression:

$$\Delta\delta^{18}O_{G.\ scitula} = -0.258(\pm0.174)t + 1.52(\pm1.00) \times (1 - \Omega_{calcite}) + 3.13(\pm0.789), \quad (4)$$

$$n = 18, \qquad r^2 = 0.63, \qquad p < 0.01.$$

The $\Delta\delta^{18}O_{G.\ scitula}$–$t$ plot corrected by substituting in situ $1 - \Omega_{calcite}$ into Eq. (4) falls on the extrapolated $\Delta\delta^{18}O_{G.\ bulloides}$–$t$ relationship with correction of $[CO_3^{2-}]$ effect (Bemis et al., 1998) (Fig. 7).

The relationship between $\Delta\delta^{18}C_{G.\ scitula}$ and $1 - \Omega_{calcite}$ (Fig. 8) is given as follows:

$$\Delta\delta^{13}C_{G.\ scitula} = 1.83(\pm1.13)(1 - \Omega_{calcite}) + 0.771(\pm0.329), \quad (5)$$

$$n = 16, \qquad r^2 = 0.46, \qquad p < 0.01.$$

Correlation coefficients for Eqs. (4) and (5) are not worse than the earlier equations using the carbonate term, although the calcite saturation term is determined by $[Ca^{2+}]$, temperature and pressure in addition to $[CO_3^{2-}]$. Certainly, the dissolution effect cannot be separated from the $[CO_3^{2-}]$ effect because the calcite saturation term itself includes $[CO_3^{2-}]$ term and largely depends on $[CO_3^{2-}]$ (see Appendix B). Even so, considering morphological variations and habitat depth of *Globorotalia scitula*, we infer the dissolution effect can partly represent the apparent $[CO_3^{2-}]$ effect found in Eqs. (2) and (3). Therefore, we propose the

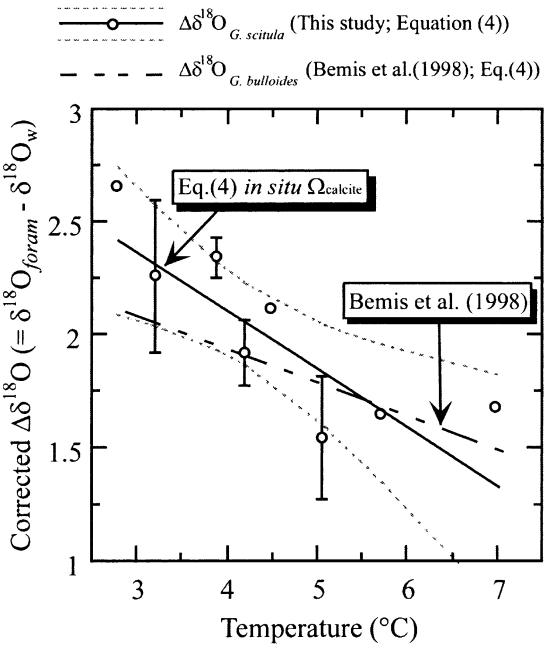

Fig. 7. (a) $(1 - \Omega_{calcite})$-corrected $\Delta\delta^{18}O(= \delta^{18}O_{G.\ scitula} - \delta^{18}O_w)$ values (‰ VPDB scale) vs. temperature for MOCNESS samples (250–500 μm size fraction; open circle). Regression line (solid line) represents $(1 - \Omega_{calcite})$-corrected $\Delta\delta^{18}O_{G.\ scitula}$:$t$ relationship (Eq. (4)) obtained for each individual with 95% interval estimate (dotted lines). Error bars represent ± standard error of the mean. Published equation provided by Bemis et al. (1998) for *G. bulloides* in consideration of $[CO_3^{2-}]$ effect $(\delta^{18}O_{G.\ bulloides} - \delta^{18}O_w = -0.204t + 2.70 + 0.005(177 - [CO_3^{2-}]_{in\ situ})$ is presented for reference (broken line).

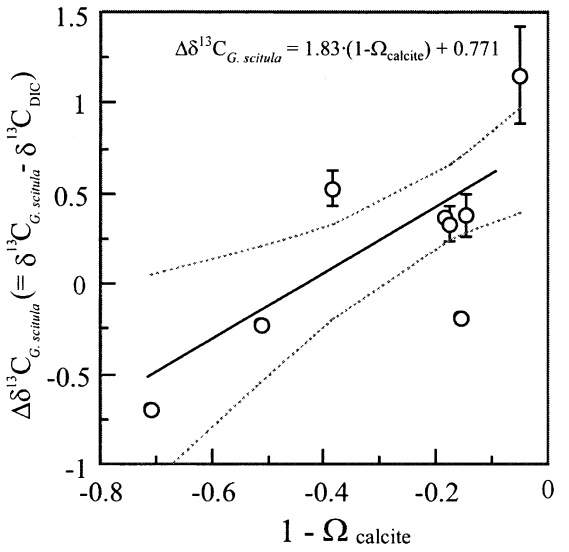

Fig. 8. $\Delta\delta^{13}C$ (‰ VPDB scale) vs. calcite saturation state of ambient water (Ω_{cal}). The $\Delta\delta^{13}C$ for each MOCNESS tow depth resolution are plotted. Dotted lines represent 95% interval estimate for the Equation (5). Total carbonate and total alkalinity were directly measured at each MOCNESS tow station, and then carbonate ion concentration and Ω_{cal} were calculated. Dissociate coefficients used in the calculation are listed in Appendix A. Error bars represent ± standard error of the mean. Regression line was generated using isotopic composition of each specimen.

$\Omega_{calcite}$ as an accommodative term to correct isotopic disequilibria in *G. scitula*, even though whichever correction terms (i.e. $[CO_3^{2-}]$ or $\Omega_{calcite}$) was chosen, corrected isotopic values may not be different.

7.4. Calibration of paleotemperature equation with time-series data

We test the newly generated paleotemperature Eq. (4) based on the result for time-series sediment trap observation. The equilibrium $\delta^{18}O_{G.\ scitula}$ value at Sta. B is predicted by substituting $\delta^{18}O_w$, temperature and $\Omega_{calcite}$ in Eq. (4).

When the Oyashio current, of which vertical temperature profile is relatively uniform, dominated at Sta. B, *Globorotalia scitula* mostly calcified at a relatively shallower depth (Figs. 2 and 9). On the other hand, when the Kuroshio-derived warm core rings were distributed over the Sta. B, *G. scitula* descended to the boundary between warm surface water mass and cold deep water (Figs. 2 and 9). Since the isopycnal depth in the Oyashio was shallower than that in warm core rings, *G. scitula* might select the $26.6–27.5\sigma_\theta$ isopycnal layers, though the habitat depth was fluctuated seasonally from 100–1200 m (Figs. 2 and 9). This is consistent with the evidence that the standing stock maximum appeared around $26.7–27.3\sigma_\theta$ based on plankton tow observations by using MOCNESS. In addition, most *G. scitula* individuals are collected around $26.5–27.2\sigma_\theta$ in the eastern Pacific (Ortiz et al., 1996). As far as temperature is concerned, throughout our sediment trap experiment *G. scitula* seemed to dwell around the depths where the temperature range is 2–5°C (Figs. 2 and 9). In spite of frequent replacement of water masses at Sta. B, this result agrees well with the result of MOCNESS (Table 2). Also, *G. scitula* calcified around the salinity minimum layer, which

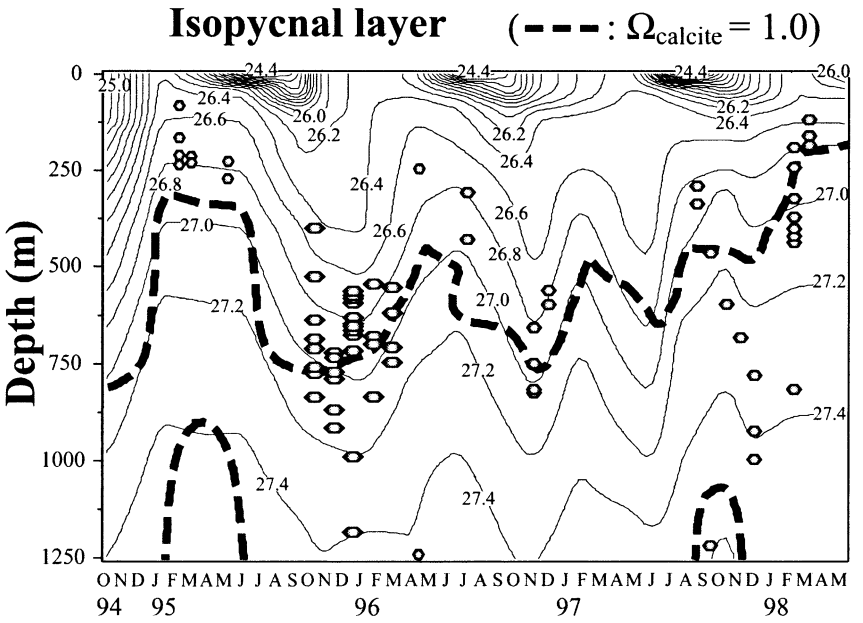

Fig. 9. Temporal variation of dwelling depth of *Globorotalia scitula* at Sta. B plotted onto isopycnals (σ_θ) on which calcite saturation horizon ($\Omega_{cal} = 1.0$) is superimposed (dotted line).

represents the NPIW. This agreement in the range of temperature, salinity and water density with the MOCNESS tow data indicate that the Eq. (4) is valid and that *G. scitula* can provide a reliable proxy for the sub-intermediate water (Figs. 2, 4 and 9).

7.5. Validity of pore dissolution hypothesis

The porosity–calcite saturation state ($\Omega_{calcite}$) relationship found in MOCNESS samples was calibrated with sediment trap samples at the predicted habitat depth using $\delta^{18}O_{G.\ scitula}$ and $\Omega_{calcite}$. Shell porosity of sediment trap samples increase from 20 to 35% with decreasing degree of calcite saturation from 1.3 to 0.9. Shell porosity on *Globorotalia scitula* collected with sediment trap was higher than MOCNESS samples (Fig. 6). The calcite saturation depth in the northern North Pacific has a minimum above 500 m, and this layer becomes shallower toward north (Wong and Matear, 1995). Regardless of the wide time and spatial resolutions of sediment trap observations, the porosity–$\Omega_{calcite}$ relationship was consistent with that of MOCNESS results. This pore morphological result of sediment trap samples sustains our dissolution hypothesis, which also explains isotopic results. Thus, the effect of shell dissolution along with pore enlargement and isotopic disequilibria in 'living' *G. scitula* can be reasonably explained.

8. Conclusions

In this study, we suggest that (1) the shell abundance in sediment core will provide information on fine suspended particle transport to sub-intermediate water, which may be related to surface water convection; (2) the calcite saturation state in the surrounding water could affect both isotopic and morphologic imprints of *Globorotalia scitula*.

Acknowledgements

We thank the captains and crews of *R/V Hokusei-Maru* and *R/V Hakuho Maru* for deployment and recovery of the sediment trap moorings. We thank the officers and crew of *R/V Soyo Maru*. We are grateful to Tadafumi Ichikawa and Kaoru Nakata, who helped with MOCNESS operation, and to Katsuyuki Sasaki, who provided the phosphate data. Thanks are

also extended to Sadamu Yamagata for operating the scanning electronic microphotograph. We also thank Kozo Okuda who cooperated with the extraction of $\sum CO_2$ for carbon isotope analysis. We express our best appreciation to Joseph D. Ortiz and Noriyuki Tanaka for their valuable comments and suggestions. The text was improved by insightful reviews from D.W. Lea and an anonymous reviewer. The research was financially supported by the Sasakawa Scientific Research Grant from the Japan Science Society.

Appendix A

A.1. Oceanographic data set at sediment trap mooring site

Based on CTD/Rosette data from oceanic observation report of the Hakodate marine observatory of the JMA, $\delta^{18}O$ of water ($\delta^{18}O_w$), total alkalinity, $\sum CO_2$ and $\delta^{13}C_{DIC}$ is estimated in the following formulas, which has been obtained empirically using observational data during SY9705 and SY9708 cruises. Note that generated formulas are valid only in the examined oceanic region.

A.1.1. The oxygen isotopes in seawater

Since the regional $\delta^{18}O_w$–salinity relationship is linearly correlated, $\delta^{18}O_w$ can be estimated using salinity. The relationship in the upper water column ($\sigma_\theta < 27.0$) is

$$\delta^{18}O_w = 0.565(\text{salinity}) - 19.4‰$$

$$r^2 = 0.94,\ n = 42,\ p < 0.01.$$

The following relationship is used for denser water ($\sigma_\theta > 27.0$)

$$\delta^{18}O_w = 0.247(\text{salinity}) - 8.65‰$$

$$r^2 = 0.64,\ n = 26,\ p < 0.01.$$

Fig. A1 shows the obtained $\delta^{18}O$–salinity relationship.

A.1.2. $\sum CO_2$ and total alkalinity

The estimated total dissolved carbon ($\sum CO_2 = [HCO_3^-] + [CO_3^{2-}] + [CO_2]$) and total alkalinity ($Alk_T = [HCO_3^-] + 2[CO_3^{2-}] + [HBO_3^-]$) in seawater using multiple linear regression analysis with four

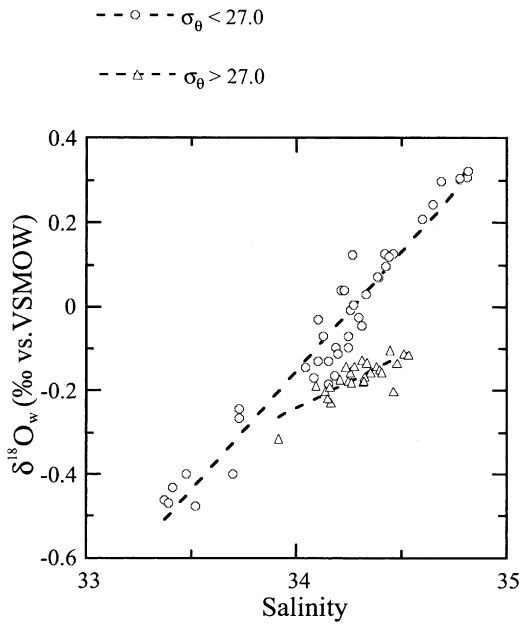

Fig. A1. The salinity–$\delta^{18}O_w$ relationship for (a) $\sigma_\theta > 27.0$ (open diamond) and (b) $\sigma_\theta < 27.0$ (circle) in the study area.

variables are expressed in the following form:

$$Alk_T = f_1(T, S, NO_3^-, AOU) \quad \text{and}$$

$$\sum CO_2 = f_2(T, S, NO_3^-, AOU).$$

Here T, S, NO_3^- and AOU represent temperature, salinity, nitrate and AOU, respectively. In this paper water with temperature below 5°C at 100 m is regarded as the Oyashio, and the other water masses were regarded as Kuroshio–Oyashio Mixed Water. Regressions for $\sigma_\theta < 26.7$ are separately calculated for the Oyashio Water and the Kuroshio–Oyashio Mixed Water.

$\sigma_\theta > 26.7$

$$Alk_T = -10.1T + 157S - 0.031NO_3^- - 0.166AOU - 2960$$

$$r^2 = 0.98,\ n = 69,\ p < 0.01,$$

$$\sum CO_2 = -5.78T + 83.9S + 4.26NO_3^- - 0.170AOU - 740$$

$$r^2 = 0.98,\ n = 69,\ p < 0.01.$$

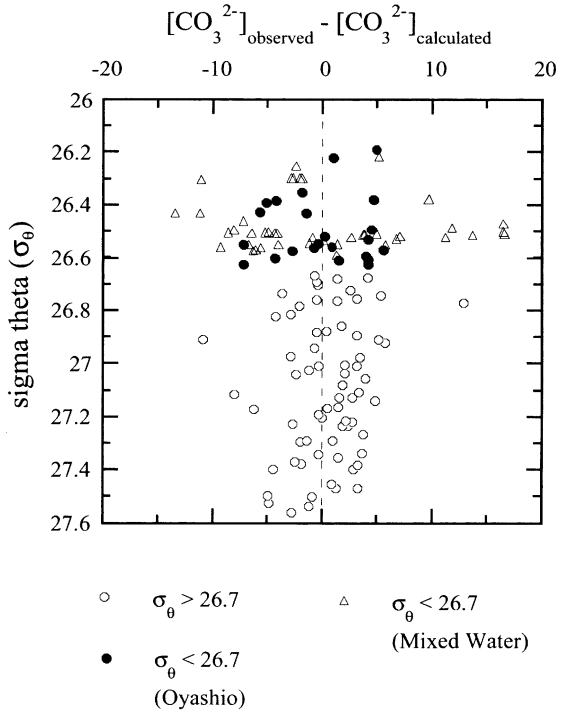

Fig. A2. Scatter plot of the $[CO_3^{2-}]$ residuals vs. σ_θ. (a) $\sigma_\theta > 26.7$ (open diamond), standard deviation of the residuals, $\sigma_R = 6$; (b) $\sigma_\theta < 26.7$ at the Oyashio Water region (closed circle), $\sigma_R = 4$; (c) $\sigma_\theta < 26.7$ at the Kuroshio–Oyashio MWR (triangle), $\sigma_R = 8$.

$\sigma_\theta > 26.7$.

For the Oyashio Water Region,

$$\mathrm{AlK_T} = -10.9\mathrm{T} + 77.1\mathrm{S} - 0.523\mathrm{NO_3^-} - 0.168\mathrm{AOU} - 268$$

$$r^2 = 0.71,\ n = 23,\ p < 0.01,$$

$$\sum \mathrm{CO_2} = -8.35\mathrm{T} + 49.0\mathrm{S} + 5.71\mathrm{NO_3^-} - 0.099\mathrm{AOU} - 408$$

$$r^2 = 0.98,\ n = 23,\ p < 0.01.$$

For the Kuroshio–Oyashio MWR,

$$\mathrm{AlK_T} = 6.70\mathrm{T} - 57.6\mathrm{S} + 0.623\mathrm{NO_3^-}\,0.044\mathrm{AOU} + 4150$$

$$r^2 = 0.57,\ n = 46,\ p < 0.01,$$

$$\sum \mathrm{CO_2} = -5.81\mathrm{T} + 27.7\mathrm{S} + 4.63\mathrm{NO_3^-} - 0.060\mathrm{AOU} + 1125$$

$$r^2 = 0.96,\ n = 46,\ p < 0.01$$

An additional term, $SiO(OH)_3^-$, might be necessary to estimate carbonate concentration more accurately, as suggested by Brewer et al. (1995). However, even if $SiO(OH)_3^-$, is not considered, estimated $[CO_3^{2-}]$ do not systematically differ from the case when $SiO(OH)_3^-$ is used (Ono, unpublished data, 1999). We, therefore, did not include $SiO(OH)_3^-$ in the calculation. Dissociation coefficients to calculate carbonate ion concentration are as follows. K_0: Weiss (1974), K_1: Roy et al. (1993), K_2: Roy et al. (1993), K_b: Dickson (1990).

The residuals of the calculated $[CO_3^{2-}]$ and their standard deviations are shown in Fig. A2. The uncertainties of 4–8 μmol CO_3^{2-}/kg (1σ) are not large because even the direct measurements include the uncertainty of ± 5 μmol CO_3^{2-}/kg.

Appendix B

B.1. Calculation of calcite saturation state

The saturation state of seawater with respect to calcite (Ω_{cal}) can be calculated when temperature, salinity, pressure, calcium ion concentration and carbonate ion concentration are known.

$$\Omega_{\mathrm{cal}} = \frac{[\mathrm{Ca^{2+}}][\mathrm{CO_3^{2-}}]}{K_{\mathrm{sp}}}$$

The effect of pressure was calculated using the apparent solubility product given by Ingle et al. (1973); Culberson and Pytkowicz (1968). The calcium concentration was estimated from salinity as $[\mathrm{Ca^{2+}}] = 2.934 \times 10^{-4}$ (salinity) (Millero, 1982).

References

Archer, D., Maier-Reimer, E., 1994. Effect of deep-sea sedimentary calcite preservation on atmospheric CO_2 concentration. Nature 367, 260–263.

Baumfalk, Y.A., Troelstra, S.R., Ganssen, G., van Zanen, M.J.L., 1987. Phenotypic variation of *Globorotalia scitula* (foraminifera)

as a response to Pleistocene climatic fluctuation. Mar. Geol. 75, 231–240.

Bé, A.W.H., 1968. Shell porosity of recent planktonic foraminifera as a climatic index. Science 161, 881–884.

Bé, A.W.H., 1977. An ecological, zoogeographic and taxonomic review of recent planktonic foraminifera. In: Ramsay, A.T.S. (Ed.), Oceanic Micropaleontology. Academic Press, London, pp. 1–100.

Bé, A.W.H., Tolderlund, D.S., 1971. Distribution and ecology of living planktonic foraminifera in surface waters of the Atlantic and Indian Oceans. In: Funnell, B.M., Riedel, W.R. (Eds.), The Micropalaeontology of Oceans. Cambridge University Press, Cambridge, pp. 105–149.

Bé, A.W.H., Harrison, S.M., Lott, L., 1973. Orbulina universa d'Orbigny in the Indian Ocean. Micropaleontology 19, 87–106.

Belyaeva, N.V., Burmistrova, I.I., 1998. The history of circulation in the Sea of Okhotsk during the late Pleistocene–Holocene as evidenced by foraminifers. Stratigr. Geol. Correl. 6, 596–603.

Bemis, B.E., Spero, H.J., Bijma, J., Lea, D.W., 1998. Reevaluation of the oxygen isotopic composition of planktonic foraminifera: Experimental results and revised paleotemperature equations. Paleoceanography 13, 150–160.

Bemis, B.E., Spero, H.J., Lea, D.W., Bijma, J., 2000. Temperature influence on the carbon isotopic composition of *Orbulina universa* and *Globigerinoides bulloides* (planktonic foraminifera). Mar. Micropaleontol. 38, 213–228.

Berger, W.H., Killingley, J.S., 1977. Glacial–Holocene transition in deep-sea carbonates: selective dissolution and the Stable isotope signal. Science 197, 563–566.

Bijma, J., Faber Jr., W.W., Hemleben, C., 1990. Temperature and salinity for growth and survival of some planktonic foraminifers in laboratory cultures. J. Foraminiferal Res. 20, 95–116.

Bijma, J., Spero, H.J., Lea, D.W., 1998. Oceanic carbonate chemistry and foraminiferal isotopes: new laboratory results. Prog. Abst. 6th Int. Conf. Paleoceanography, p. 78.

Bouvier-Soumagnac, Y., Duplessy, J.-C., 1985. Carbon and oxygen isotopic composition of planktonic foraminifera from laboratory culture, plankton tows and recent sediment: implications for the reconstruction of paleoclimatic conditions and of the global carbon cycle. J. Foraminiferal Res. 15, 302–320.

Brewer, P.G., Glover, D.M., Goyet, C., Shafer, D.K., 1995. The pH of the North Atlantic Ocean: improvements to the global model for sound absorption in seawater. J. Geophys. Res. 100, 8761–8776.

Coplen, T.B., 1996. More uncertainty than necessary. Paleoceanography 11, 369–370.

Culberson, C.H., Pytkowicz, R.M., 1968. Effect of pressure on carbonic acid, boric acid and the pH in sea water. Limnol. Oceanogr. 13, 403–417.

Dickson, A.G., 1990. Thermodynamics of the dissociation of boric acid in synthetic seawater from 273.14 to 318.15K. Deep-Sea Res. 37, 755–766.

Erez, J., Luz, B., 1983. Experimental paleotemperature equation for planktonic foraminifera. Geochim. Cosmochim. Acta 47, 1025–1031.

Fairbanks, R.G., Wiebe, P.H., 1980. Foraminifera and chlorophyll maximum: vertical distribution, seasonal succession, and paleoceanographic significance. Science 209, 1524–1526.

Frerichs, W.E., Heiman, M.E., Leon, E., Borgman, L.E., Be, A.W.H., 1972. Latitudinal variation in planktonic foraminiferal test porosity: part 1.Optical studies. J. Foraminiferal. Res. 2, 6–13.

Hecht, A.D., Bé, A.W.H., Lott, L., 1976. Ecologic and paleoclimatic implications of morphologic variation of Orbulina universa in the Indian Ocean. Science 194, 422–424.

Hemleben, C., Bijma, J., 1994. Foraminiferal population dynamics and stable carbon isotopes. In: Zahn, R., Pedersen, T.F., Kaminski, M.A., Labeyrie, L. (Eds.), Carbon Cycling in the Glacial Ocean: Constraints on the Ocean's Role in Global Change. Springer, Berlin, pp. 145–166.

Hemleben, C., Bé, A.W.H., Andersen, O.R., Tuntivate, S., 1977. Test morphology, organic layers and chamber formation of the planktonic foraminifer *Globorotalia menardii* (d'Orbigny). J. Foraminiferal. Res. 7, 1–25.

Hemleben, C., Spindler, M., Anderson, O.R., 1989. Modern Planktonic Foraminifera. Springer, New York.

Hendy, I.L., Kennett, J.P., 2000. Dansgaard-Oeschger cycles and the California current system: planktonic foraminiferal response to rapid climate change in Santa Barbara Basin, ocean drilling program hole 893A. Paleoceanography 15, 30–42.

Hutson, W.H., 1977. Variations in planktonic foraminiferal assemblages along north-south transects in the Indian ocean. Mar. Micropaleontol. 2, 47–66.

Ingle, S.E., Culberson, C.H., Hawley, J.E., Pytkowitcz, R.M., 1973. The solubility of calcite in sea water at atmospheric pressure and 35% salinity. Mar. Chem. 1, 295–307.

Jorissen, F.J., 1999. Benthic foraminiferal successions across Late Quaternary Mediterranean sapropels. Mar. Geol. 153, 91–101.

Kahn, M.I., Williams, D.F., 1981. Oxygen and carbon isotopic composition of living planktonic foraminifera from the Northwest Pacific ocean. Palaeogeogr. Palaeoclimatol. Palaeoecol. 33, 47–69.

Keigwin, L.D., 1998. Glacial-age hydrography of the far northwest Pacific Ocean. Paleoceanogaphy 13, 323–339.

Kwiek, P.B., Ravelo, A.C., 1999. Pacific Ocean intermediate and deep water circulation during Pliocene. Paleogeogr., Paleoclimatol., Paleoecol. 154, 197–217.

Lohmann, G.P., Schweitzer, P.N., 1990. Globorotalia truncatulinoides growth and chemistry as probes of the past thermocline: 1. Shell size. Paleoceanography 5, 55–75.

Lynch-Stieglitz, J., Fairbanks, R.G., 1994. A conservative tracer for glacial ocean circulation from carbon isotope and paleonutrient measurements in benthic foraminifera. Nature 369, 308–310.

Lynch-Stieglitz, J., van Geen, A., Fairbanks, R.G., 1996. Interocean exchange of Glacial North Atlantic Intermediate Water: evidence from Subantarctic Cd/Ca and carbon isotope measurements. Paleoceanography 11, 191–201.

Marchant, M., Hebbeln, D., Wefer, G., 1998. Seasonal flux pattern of planktonic foraminifera in the Peru–Chile current. Deep-Sea Res. 45, 1161–1185.

Marchitto Jr., T.M., Curry, W.B., Oppo, D.W., 1998. Millennial-scale changes in North Atlantic circulation since the last glaciation. Nature 393, 557–561.

Martin, J.H., 1990. Glacial–Interglacial CO_2 change: the iron hypothesis. Paleoceanography 5, 1–13.

Millero, F.J., 1982. The thermodynamics of seawater at one atmosphere. Ocean. Sci. Eng. 7, 403–460.

Milliman, J.D., Troy, P.J., Balch, W.M., Adams, A.K., Li, Y.-H., Mackenzie, F.T., 1999. Biologically mediated dissolution of calcium carbonate above the chemical lysocline? Deep-Sea Res. 46, 1653–1669.

Morse, J.W., 1974. Dissolution kinetics of calcium carbonate in solution: V. Effects of natural inhibitors and the position of the chemical lysocline. Amer. J. Sci. 272, 840–851.

Mulitza, S., Arz, H., von Mücke, S.K., Moos, C., Niebler, H.-S, Pätzold, J., Segl, M., 1999. The South Atlantic carbon isotope record of planktonic foraminifera. In: Fisher, G., Wefer, G. (Eds.), Use of Proxies in Paleoceanography, pp. 427–445.

Noriki, S., Saito, C., Tsunogai, S., 1990. A simple indirect method for the determination of organic-carbon in marine particles. J. Oceanogr. Soc. Japan 46, 135–138.

Noriki, S., Iwai, T., Shimamoto, A., Tsunogai, S., Harada, K., 1995. Spatial variation of Al flux in the North Pacific observed with sediment trap. In: Sakai, H., Nozaki, K. (Eds.), Biogeochemical Processes and Ocean Flux in the Western Pacific. Scientific Publishing Company, Tokyo, pp. 345–354.

Oba, T., 1988. Paleoceanographic information obtained by the isotopic measurement of individual foraminiferal specimens. In: Wang, P., Lao, Q., He, Q. (Eds.), Proceedings of the 1st International Conference on Asian Marine Geology. China Ocean Press, Beijing, pp. 169–179.

Oba, T., Pedersen, T.F., 1999. Paleoclimatic significance of eolian carbonates supplied to the Japan Sea during the last glacial maximum. Paleoceanography 14, 34–41.

Ono, T., Sasaki, K., 2000. Seasonal transition in the distributions of carbonate properties and nutrients in the Kuroshio/Oyashio Interfrontal Zone observed during January to August 1997. Bull. Natl. Inst. Fish. Sci. 14, 9–38.

Ortiz, J.D., Mix, A.C., 1992. The spatial distribution and seasonal succession of planktonic foraminifera in the California Current off Oregon, September 1987–1988. In: Summerhayes, C.P., Prell, W.L., Emeis, K.C. (Eds.), Upwelling Systems: Evolution Since the Early Miocene, Geological Society London Special Publication, 197–213.

Ortiz, J.D., Mix, A.C., Collier, R.W., 1995. Environmental control of living symbiotic and asymbiotic foraminifera of the California Current. Paleoceanography 10, 987–1009.

Ortiz, J.D., Mix, A.C., Watkins, J.M., Collier, R.W., 1996. Deep-dwelling planktonic foraminifera of the northeastern Pacific Ocean reveal environmental control of oxygen and carbon isotopic disequilibria. Geochim. Cosmochim. Acta 60, 4509–4523.

Parker, F.L., Berger, W.H., 1971. Faunal and solution patterns of planktonic foraminifera in surface sediments of the South Pacific. Deep-Sea Res. 18, 73–107.

Petit, J.R., Jouzel, J., Raynaud, D., Barkov, N.I., Barnola, J.-M., Basile, I., Bender, M., Chapellaz, J., Davis, M., Delaygue, G., Delmotte, M., Kotlyakov, V.M., Legrand, M., Lipenkov, V.Y., Lorius, C., Pépin, L., Ritz, C., Saltzman, E., Stievenard, M., 1999. Climate and atmospheric history of the past 420,000 years from the Vostok ice core, Antarctica. Nature 399, 429–435.

Reid, J.L., 1965. Intermediate waters of the North Pacific Ocean. The Johns Hopkins Oceanographic Studies. 85 pp.

Reynolds, L., Thunell, R.C., 1985. Seasonal succession of planktonic foraminifera in the subpolar North Pacific. J. Foraminiferal. Res. 15, 282–301.

Romanek, C.S., Grossman, E.L., et al., 1992. Carbon isotopic fractionation in synthetic aragonite and calcite: Effects of temperature and precipitation rate. Geochim. Cosmochim. Acta 56, 419–430.

Roy, R.N., Roy, L.N., Vogel, K., Moore, C.P., 1993. Determination of the ionization constants of carbonic acid in seawater. Mar. Chem. 44, 249–268.

Russell, A.D., Spero, H.J., 2000. Field examination of the oceanic carbonate ion effect on planktonic foraminiferal $\delta^{13}C$. Paleoceanography, 43–52.

Saino, T., 1992. ^{15}N and ^{13}C natural abundance in suspended particulate organic matter from a Kuroshio warm-core ring. Deep-Sea Res. 39, 347–362.

Sanyal, A., Hemming, N.G., Hanson, G.N., 1995. Evidence for a higher pH in the glacial ocean from boron isotopes in foraminifera. Nature 373, 234–236.

Schiebel, R., Hiller, B., Hemleben, C., 1995. Impacts of storms on recent planktic foraminiferal test production and $CaCO_3$ flux in the North Atlantic at 47°N, 20°W (JGOFS). Mar. Micropaleontol. 26, 115–129.

Shiga, K., Koizumi, I., 2000. Latest Quaternary oceanographic changes in the Okhotsk Sea based on diatom records. Mar. Micropaleontol. 38, 91–117.

Spero, H.J., Lea, D.W., 1996. Experimental determination of Stable isotope variability in Globigerina bulloides: implications for paleoceanographic reconstructions. Mar. Micropaleontol. 28, 231–246.

Spero, H.J., Bijma, J., Lea, D.W., Bemis, B.E., 1997. Effect of seawater carbonate concentration on foraminiferal carbon and oxygen isotopes. Nature 390, 497–500.

Sverdrup, H., Johnson, M.W., Fleming, R.H., 1942. The Oceans: Their Physics, Chemistry, and Biology. Prentice-Hall, Engelwood Cliffs, NJ, p. 1087.

Tally, L.D., 1991. An Okhotsk Sea water anomaly: implications for ventilation in the North Pacific. Deep-Sea Res. 38, 171–190.

Thompson, P.R., 1981. Planktonic foraminifera in the western north Pacific during the past 150,000 years: Comparison of modern and fossil assemblages. Palaeogeogr. Palaeoclimatol. Palaeoecol. 35, 241–279.

Thunell, R.C., 1978. Distribution of recent planktonic foraminifera in surface sediments of the Mediterranean Sea. Mar. Micropaleontol. 3, 147–173.

Thunell, R.C., Reynolds, L.A., 1984. Sedimentation of planktonic foraminifera: seasonal changes in species flux in the Panama Basin. Micropaleontology 30, 243–262.

Troy, P.J., Li, Y.-H., Mackenzie, F.T., 1997. Changes in surface morphology of calcite exposed to the oceanic water column. Aquatic Geochem. 3, 1–20.

Watkins, J.M., Mix, A.C., Wilson, J., 1996. Living planktonic foraminifera: tracers of circulation and productivity regimes in the central equatorial Pacific. Deep-Sea Res. II 43, 1257–1282.

Weiss, R., 1974. Carbon dioxide in water and seawater. The solubility of a non-ideal gas. Mar. Chem. 2, 203–215.

Wiebe, P.H., Burt, K.H., Boyd, S.H., Morton, A.W., 1976. A multiple opening/closing net and environmental sensing system for sampling zooplankton. J. Mar. Res. 34, 313–326.

Wong, C.S., Matear, R., 1995. Fate and effects of disposed CO_2 for scenarios in the North Pacific Ocean. In: Handa, Ohsumi (Eds.), Direct Ocean Disposal of Carbon Dioxide. Terrapub, Tokyo, pp. 103–122.

Yasuda, I., 1997. The origin of the Pacific Intermediate Water. J. Geophys. Res. 102, 893–909.

Yasuda, I., Okuda, K., Hirai, M., Ogawa, Y., Kudoh, H., Fukushima, S., Mizuno, K., 1988. Short-term variations of the Tsugaru Warm Current in autumn. Bull. Tohoku Region Fish. Res. Lab. 50, 153–191.

Yasuda, I., Okuda, K., Hirai, M., Ogawa, Y., Kudoh, H., Fukushima, S., Mizuno, K., 1992. Evolution of a Kuroshio warm-core ring: Variability of the hydrographic structure. Deep-Sea Res. 39, S131–S161.

Yasuda, I., Okuda, K., Shimizu, Y., 1996. Distribution and modification of North Pacific Intermediate Water in the Kuroshio-Oyashio interfrontal zone. J. Phys. Oceanogr. 26, 448–465.